



Identification of novel antitubercular compounds through hybrid virtual screening approach

Muhammad Muddassar^{a,b}, Jae Wan Jang^{a,b}, Hong Seung Gon^c, Yong Seo Cho^a, Eunice Eunkyung Kim^a, Kyo Chang Keum^a, Taegwon Oh^c, Sang-Nae Cho^c, Ae Nim Pae^{a,*}

^a Center for Chemoinformatics Research, Life Sciences Division, Korea Institute of Science and Technology, PO Box 131, Cheongryang, Seoul 130-650, Republic of Korea

^b School of Science, University of Science and Technology, 52 Eoeun dong, Yuseong-gu, Daejeon 305-333, Republic of Korea

^c Department of Microbiology and the Brain Korea 21 Project for the Medical Sciences, Yonsei University College of Medicine, Seoul 120-752, Republic of Korea

ARTICLE INFO

Article history:

Received 27 April 2010

Revised 2 July 2010

Accepted 3 July 2010

Available online 18 August 2010

Keywords:

Mycobacterium tuberculosis

Antimicrobial agents

Ligand based

Structure based

Virtual screening

ABSTRACT

Growing resistance of prevalent antitubercular (antiTB) agents in clinical isolates of *Mycobacterium tuberculosis* (MTB) provoked an urgent need to discover novel antiTB agents. Enoyl acyl carrier protein (ACP) reductase (InhA) from Mtb is a well known and thoroughly studied as antitubercular therapy target. Here we have reported the discovery of potent antiTB agents through ligand and structure based approaches using computational tools. Initially compounds with more than 0.500 Tanimoto similarity coefficient index using functional class fingerprints (FCFP₄) to the reference chemotype were mined from the chemdiv database. Further, the molecular docking was performed to select the compounds on the basis of their binding energies, binding modes, and tendencies to form reasonable interactions with InhA (PDB ID = 2NSD) protein. Eighty compounds were evaluated for antitubercular activity against H37RV *M. tuberculosis* strain, out of which one compound showed MIC of 5.70 μ M and another showed MIC of 13.85 μ M. We believe that these two new scaffolds might be the good starting point from hit to lead optimization for new antitubercular agents.

© 2010 Elsevier Ltd. All rights reserved.

1. Introduction

Tuberculosis (TB), a lung infection caused mainly by *Mycobacterium tuberculosis* (MTB), is one of the threatening and wide spreading infectious diseases in the world.¹ According to world health organization (WHO) reports one-third of the world's population is supposed to be latently infected by MTB with high death toll in developing countries. Despite the alarming spread of tuberculosis to the public, no sufficiently effective and promising antitubercular agents have been launched into the pharmaceutical market over the past many years. Till date isoniazid (INH), pyrazinamide, ethambutol, and rifampicin are considered as promising treatment drugs against the MTB infection.^{2,3} Many published reports^{2–4} on the resistance of these agents against the virulence strains of MTB incite the researchers to develop the antiTB agents on the priority basis.⁵

Recently many attractive targets have been identified for the design and development of new generation antitubercular agents.⁶ The NADH-dependent enoyl-ACP reductase of MTB (also known as InhA) encoded by the mycobacterium InhA gene has been validated as the primary molecular target for frontline and second line antitubercular agents.⁷ InhA catalyzes the reduction of long-chain *trans*-2-enoyl-ACP in the type II fatty acid biosynthesis pathway

of *M. tuberculosis*.⁸ Inhibition of InhA terminates the biosynthesis of the mycolic acids that are the primary constituents of mycobacterial cell wall. INH and ethionamide (ETA) activates through the intermediate complex formation by catalase-peroxidase (Kat G) and (EtaA) flavoprotein monooxygenase, respectively.^{9,10} Clinical isolates have revealed that mutations that occurred in the genes of both the enzymes in MTB cause the resistance against these prevalent drugs. However, several classes of compounds like arylamide, diarylether, triclosan derivatives, and pyrrolidine carboxamides that directly bind to InhA without acquiring activation through this mechanism have either been synthesized or acquired by high throughput virtual screening.^{11–14}

In the present study we have identified the novel antitubercular agents from large chemical database using computational techniques. We have used the hybrid virtual screening approach in which both ligand based¹⁵ as well as structure-based informations¹⁶ were used to mine the antiTB compounds from chemdiv database. In the first step we have performed a similarity search of different chemotypes nanomolar active compounds, directly binding to InhA, from commercially available database. While in the second step the molecular docking simulations on the closest similarities of these compounds were carried out. Starting from 693,042 structures, we selected, purchased, and tested 80 compounds for antibacterial activity against *M. tuberculosis* H37Rv strain which resulted in two novels antitubercular hits.

* Corresponding author. Tel.: +82 2 958 5185; fax: +82 2 958 5189.

E-mail address: anpae@kist.re.kr (A.N. Pae).

2. Materials and methods

2.1. Data set preparation

To identify the novel and potent antiTB agents from the small molecules chemdiv database, three different chemotypes (Fig. 1) compounds were collected from the literature,^{11–14} which have <1 μM InhA inhibitory concentration. The chemotypes were defined on the basis of two factor, firstly each type must have novel central scaffold of directly binding InhA inhibitors and secondly one of its ligand should be a co-crystal with fabI enzyme of *M. tb*. The molecular construction and modeling of these query ligands were performed using the molecules building tools available in maestro 9.0.111 (Schrodinger Inc.). These ligands were minimized using the OPLS 2005 force field.

We also prepared the database by adding hydrogen atoms and rectification of wrong valences in its compounds. For molecular docking simulations of similarity search based retrieved 531 hit compounds, we first used LigPrep module implemented in our molecular modeling Schrodinger package. This 2D to 3D conversion program generates accurate energy minimized molecular structures with their tautomeric structures, ionization states, ring conformations, and stereoisomers to produce broad chemical and structural diversity from a single input structure. The compounds were only restricted to 3D structure generation and their ionization states at physiological pH by retaining their original chirality.

2.2. Ligand-based similarity search

In similarity search of highly active compounds of the reported antibacterial agents against *M. tuberculosis*, the Tanimoto similarity indices for the reference compounds were calculated using SciTe-gic functional class fingerprints (FCFP_4) in Pipeline Pilot 7.4.¹⁷ FCFPs encode the atomic environments of six generalized atom types: hydrogen bond donors and acceptors; positive and negative ionizable centers; aromatic atoms and halogens. They are more closely related to substructural fingerprints than are distance based pharmacophores.¹⁸ It uses an OptiSim like algorithm to select a maximally diverse subset of a given size. The commercially available chemdiv database was screened against fabI active compounds using pipeline pilot generated FCFP_4 descriptors to identify more potent antibacterial compounds. We only collected the compounds for docking those which have more than 0.500 Tanimoto coefficient values.

2.3. Protein preparation and docking simulations

The crystal structures of fabI of *M. tuberculosis* were retrieved from the Protein Data Bank (www.rcsb.org) (PDB IDs: 2B36, 2H7L, 2NSD, and 3FNG). All crystallographic water molecules were removed from these structures as none of these were involved in

the salt bridge formation. Similarly co-crystal ligands were also removed from each crystal structure. Hydrogen atoms were added and OPLS_2005 force field-based charges were assigned. A brief minimization to relieve steric clashes was also performed using the protein preparation module in Maestro with the 'preparation and refinement' option. This restrained partial minimization was terminated when the root-mean-square deviation (rmsd) reached a maximum value of 0.3 Å. For molecular docking, we have used Glide^{20,21} module implemented in Schrodinger suit 2009 (Schrodinger, Inc.). The Amino acid residues located within 12 Å from the co-crystal ligand were defined as the possible binding site for docking simulations. A spatial constrain of carbonyl moiety was introduced towards the Tyr158 to form hydrogen bond with the docking ligand in the grid enclosing box and a scaling factor of 1.00 was set to van der Waals (VDW) radii of receptor atoms with the partial atomic charge <0.25. Similarly hydrophobic cells were also generated and incorporated in the GRID box. In the docking studies, standard precision (SP) mode was used, and the Glide scoring function (G-score) was calculated to select the best pose for each ligand. The docking simulations were performed on a multi-processor linux system.

2.4. Assay for antitubercular activity

The minimal inhibitory concentration of each compound against *M. tuberculosis* (*M. tb*) H37Rv was determined by the micro-plate alamar blue assay.¹⁹ *M. tuberculosis* was grown in 10 ml of middle brook7H9 broth (Difco, parks, MD) supplemented with 0.2% (vol/vol) glycerol (Sigma Chemical Co., Saint Louis, MO), 1.0 g of Casitone (Difco) per liter, 10% (vol/vol) OADC (oleic acid, albumin, dextrose, catalase; Difco), and 0.05% (vol/vol) tween80 (Sigma) till its optical density at 600 nm reached 0.4. Initial compound solution was prepared in dimethylsulfoxide, and two-fold serial dilutions were made in 7H9 broth in the microplates. The culture was diluted 1:50 in 7H9 and inoculated to yield 2×10^5 CFU/ml in plate wells. The plates containing compounds dilutions and MTB were incubated at 37 °C for 7 days, and then 20 μl of 10 \times alamar blue solution (Serotec, Raleigh, NC) was added to each well. The color change from blue to pink was observed after 24 h incubation, and the minimal inhibitory concentration (MIC) was defined as the lowest concentration of compounds that inhibited a color change.

3. Results and discussion

The virtual screening workflow employed in this study is similar to previously reported study²⁰ where similarity search of a ligand molecule has been used in conjunction with docking and scoring. In this hybrid virtual screening approach we used different chemotypes starting structures to identify the relatively novel scaffold with improved antibacterial activity against MTB. The strategy for the similarity search-based virtual screening was using the functional class fingerprints based weighting using Tanimoto coefficient which is commonly used for binary data, as the quantitative measure of bit string similarity. In short highly active compounds of four different chemotypes against InhA were used to screen the chemdiv small molecule database consisting of 693,042 compounds. Subsequently, the compounds with closest similarities to the reference compounds were docked and prioritized using receptor interaction information and visual inspections.

3.1. Ligand-based identification

Nowadays different ligand-based methodologies such as pharmacophore mapping and QSAR techniques are employed as a

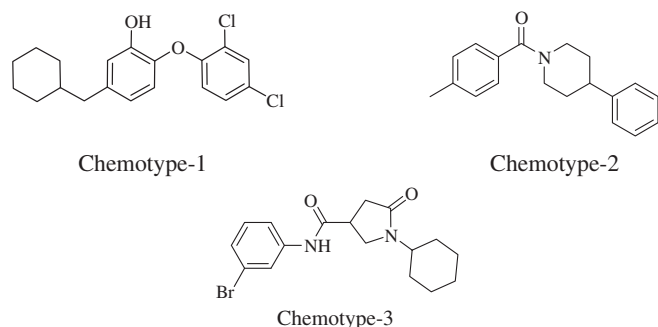


Figure 1. Different representative chemotype structures used for similarity search analysis.

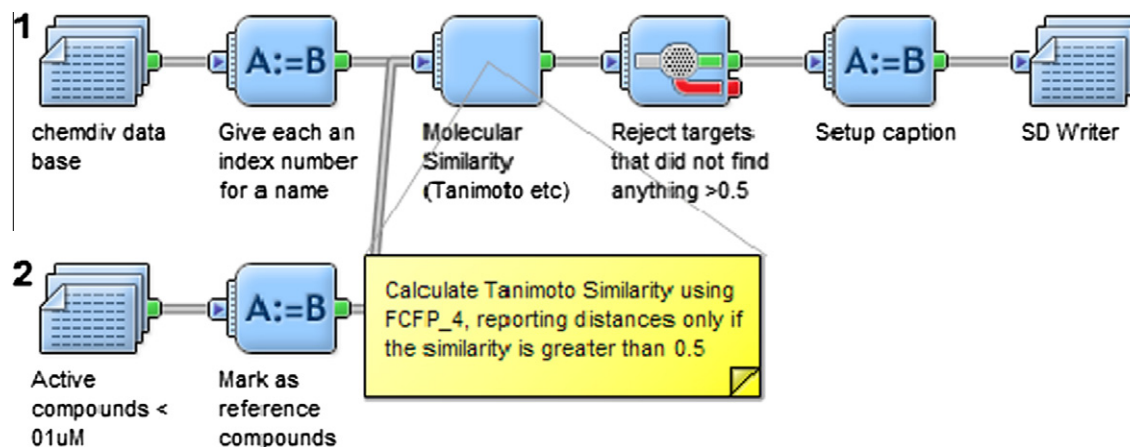


Figure 2. Pipeline pilot similarity search protocol for database screening of four different chemotypes.

primary filter to mine the chemical databases for the identification of active molecules against certain biological target. But similarity search using 2D fragment bit strings provides an effective and efficient way for virtual screening, when multiple reference structures are available. For each of the four chemotype classes shown in Figure 1, 32 active compounds with $<1 \mu\text{M}$ activity were taken in the training set. Pipeline pilot protocol (Fig. 2) for similarity search of these training set compounds yielded total 1125 hits, in which some were in duplication and others did not follow the Lipinski's rule. The hits with pairwise Tanimoto coefficient values greater than 0.500 and smaller than 0.800 were selected to avoid the inclusion of closely related analogous compounds. In this first step screening 531 hits were finally obtained after removal of duplicates and by applying drug like filter (shown in Fig. 3). The results of similarity search calculation showed that fragment consisting of conserved atoms (CO) involved in hydrogen bonding with the protein in training set ligands were most effective in detecting the new active compounds from the database, although they were smaller than entire ligand. All hits acquired this feature probably due to FCFP_4 fingerprints that encode the descriptors of hydrogen bond acceptor. The selected compounds from this filter were subjected to the molecular docking simulations to reduce their optimum number for biological assay.

3.2. Docking protocol optimization

Before carrying out the molecular docking simulations of hits obtained from similarity search, docking protocol was optimized. There are four crystal structures (2B36, 2H7L, 3FNG, and 2NSD) of InhA enzyme which are available in the protein data bank with different co-crystal ligands. All co-crystal ligands of InhA have conserved hydrogen bonding interactions with the Tyr158 and OH of ribose of NAD^+ stacked in crystal structures. On cross docking of these ligands in these protein 3D structures with Glide produced the variable binding poses with significant different binding energies in each docking run, as shown in Table 1. This might have arisen due to the induced fit mechanism of proteins which complicates cross docking of ligands from different ligand protein complexes.²¹ Figure 4 demonstrated this effect of conformational rearrangements of aliphatic side chains on crystallization of different ligands in same protein. Similarly TM-align,²² a protein topology and side chain conformational comparison tool, predicted various TM-scores and RMSDs of side chains of all protein 3D structures despite of their 100% sequence similarity, data has shown in Table 2. However 3FNG and 2NSD comparison yielded the least score difference of 0.990 TM-score and 0.653 RMSD in side chains confirmations. The pharmacophoric constrains that

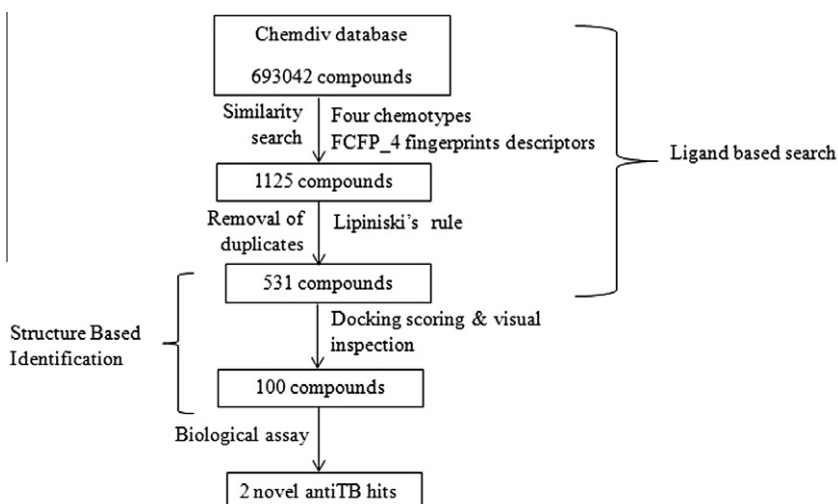
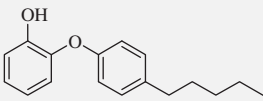
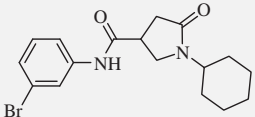
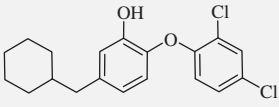
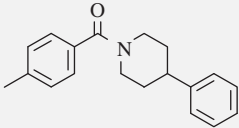


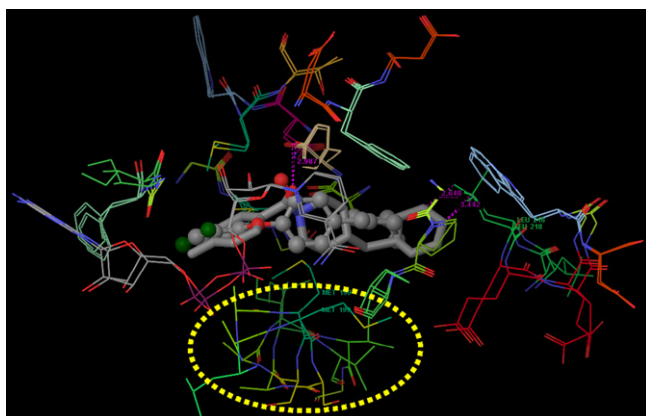
Figure 3. Virtual screening workflow for novel antitubercular agents.

Table 1

Number of constrained used, docked co-crystal ligands, and G-score values obtained in docking protocol optimization for crystal structure selection

Protocol	Co-crystal	PDB	Constrain	No. of docked ligands	G-score
1		2B36	Total = 3 (P, H, 1H-bond) Used = any 3	3	–7.03 Top ranked = 3FNG co-crystal
2		2B36	Total = 3 (P, H, 1H-bond) Used = any 2	3	–6.92 Top ranked = 3FNG co-crystal
3		2B36	No constrain used	4	–7.77 Top ranked = 2NSD co-crystal
4		2H7L	Total = 4 (P, H, 2H-bond) Used = any 3	3	–7.35 Top ranked = 2H7L co-crystal
5		2H7L	Total = 4 (P, H, 2H-bond) Used = any 2	4	–8.96 Top ranked = 2H7L co-crystal
6		2H7L	Total = 5 (P, 2H, 2H-bond) Used = any 2	4	–8.13 Top ranked = 2NSD co-crystal
7		2H7L	No constrain used	4	–9.04 Top ranked = 2H7L co-crystal
8		3FNG	Total = 4 (P, H, 2H-bond) Used = any 4	2	–8.43 Top ranked = 3FNG co-crystal
9		3FNG	Total = 4 (P, H, 2H-bond) Used = any 3	3	–8.53 Top ranked = 3FNG co-crystal
10		3FNG	Total = 4 (P, H, 2H-bond) Used = any 2	3	–8.37 Top ranked = 3FNG co-crystal
11		3FNG	Total = 4 (P, H, 2H-bond) Used = any 4	2	–8.43 Top ranked = 3FNG co-crystal
12		3FNG	No constrain used	4	–8.60 Top ranked = 3FNG co-crystal
13		2NSD	Total = 5 (P, H, 2H-bond) Used = any 3	3	–8.91 Top ranked = 3FNG co-crystal
14		2NSD	Total = 5 (P, 2H, 2H-bond) Used = any 2	4	–10.16 Top ranked = 2NSD co-crystal
15		2NSD	No constrain used	4	–10.18 Top ranked = 2NSD co-crystal

P, positional constrain; H, hydrophobic constrain.

**Figure 4.** Overlapped crystal structures 2NSD and 3FNG of same protein are demonstrating the conformational change (in yellow ring) of aliphatic side chains on binding of different ligands. Ball and sticks indicate 3FNG co-crystal ligand whereas sticks are used for 2NSD. Protein residues are represented by lines.**Table 2**

The TM-scores and RMSDs of different X-ray crystal structures of InhA protein

No.	PDB coordinates	TM-score	RMSD
1	2B36-2H7L	0.988	0.692
2	2B36-2NSD	0.982	0.978
3	2B36-3FNG	0.979	1.084
4	2H7L-2NSD	0.984	0.819
5	2H7L-3FNG	0.983	0.952
6	2NSD-3FNG	0.990	0.653

RMSD, root mean square deviation of the common residues.

defined during the GRID generation were used for each ligand–protein complex in each docking run of co-crystal ligands. Among these proteins, the 3FNG and 2NSD complexes reproduced the exact binding mode as of co-crystal ligands with lowest binding energies –8.60 kcal/mol and –10.18 kcal/mol, respectively. In these optimization studies, among all X-ray structures only 2NSD has accommodated all the ligands with

Table 3

Antitubercular activity, Tanimoto similarity coefficient index, and docking scores of newly identified hits

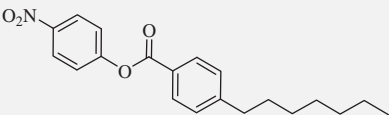
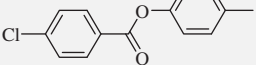
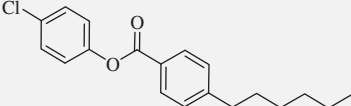
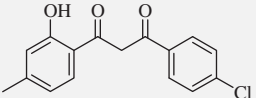
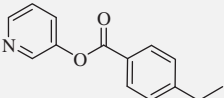
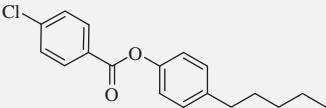
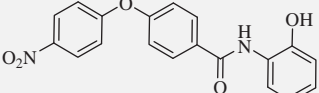
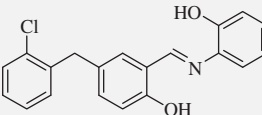
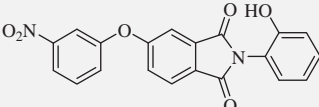
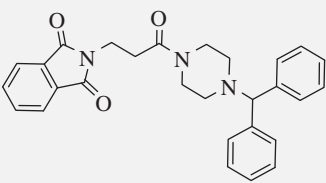
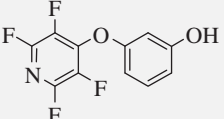
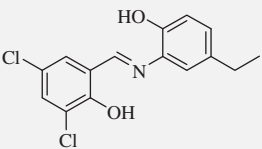
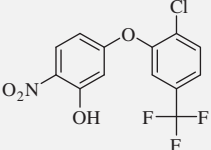
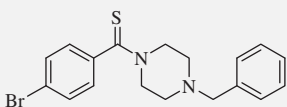
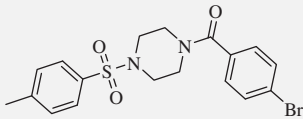
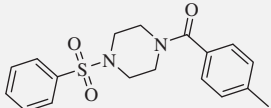
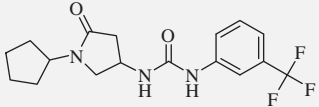
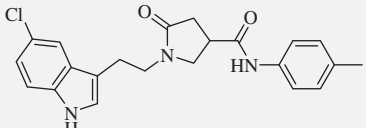
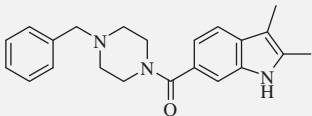
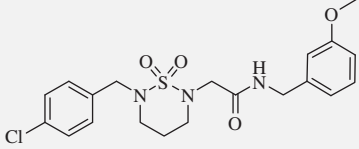
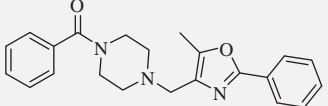
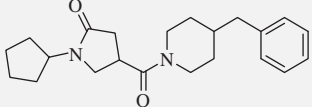
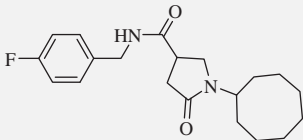
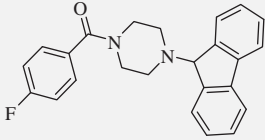
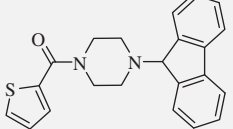
No.	ID number	Structure	MIC (μ M) H37Rv	Similarity index	G-score
1	VH01		187.40	0.60	−9.101
2	VH02		259.42	0.501	−7.107
3	VH03		202	0.540	−7.433
4	VH04		13.85	0.510	−8.751
5	VH05		563.20	0.513	−7.227
6	VH06		105.68	0.540	−8.520
7	VH07		5.70	0.555	−8.219
8	VH08		181.90	0.512	−10.039
9	VH09		85.03	0.619	−10.101
10	VH10		141.10	0.571	−11.630
11	VH11		246.95	0.510	−7.575
12	VH12		206.33	0.513	−7.000
13	VH13		383.63	0.524	−8.165

Table 3 (continued)

No.	ID number	Structure	MIC (μ M) H37Rv	Similarity index	G-score
14	VH14		85.25	0.528	−8.947
15	VH15		302.36	0.540	−8.667
16	VH16		371.61	0.656	−8.696
17	VH17		180.09	0.520	−8.788
18	VH18		80.83	0.519	−7.289
19	VH19		368.38	0.541	−9.013
20	VH20		146.13	0.516	−7.922
21	VH21		187.48	0.550	−7.843
22	VH22		361.07	0.550	−9.159
23	VH23		369.46	0.619	−10.428
24	VH24		85.91	0.788	−11.439
25	VH25		355.08	0.649	−10.911
	Control	Rifampicin	0.010		

their exact binding modes and reasonable low binding energies compared to other structures. Therefore based on these results we used 2NSD coordinates for our docking simulations of hit compounds.

3.2.1. Molecular docking studies

The hit compounds retrieved from ligand-based similarity search were subjected to isomeric analysis using Ligprep module. The protonation of these ligands generated greater number of

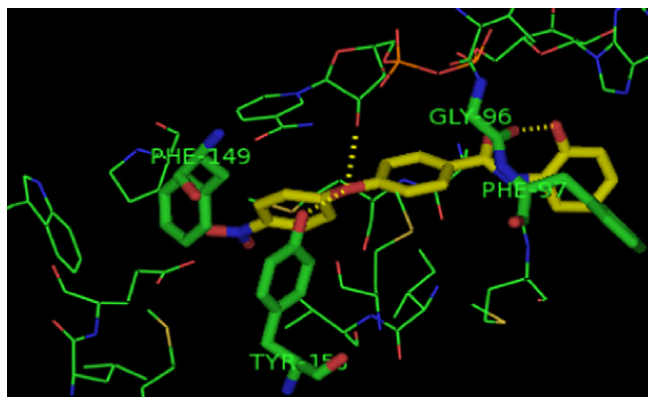


Figure 5. Predicted binding mode of VH07 hit in the 2NSD active site. The hit compound is drawn in sticks representation, where the coloring of atoms for VH07 is: carbon, yellow; nitrogen, blue; and oxygen, red. 2NSD active site residues that make hydrogen bonding are labeled and displayed in stick representations. Yellow dashed lines are showing hydrogen bonding. Figure generated with the program pymol.

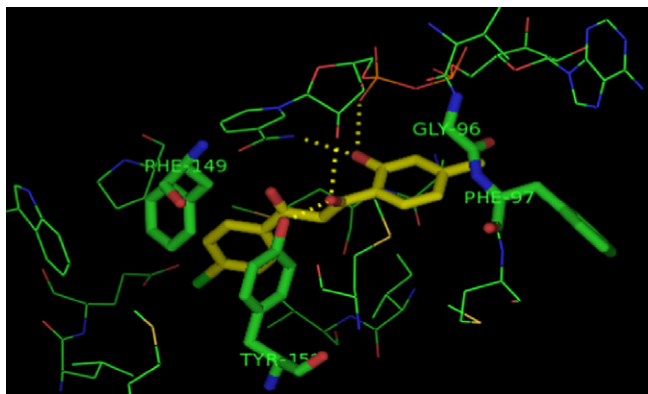


Figure 6. Predicted binding mode of VH04 hit in the 2NSD active site. The color scheme, amino acid residues, and orientation of the active site are identical to that of Figure 5.

isomers than actual number of compounds due to more than one ionization states of a compound at physiological pH. The molecular docking simulations of all these compounds were carried out in InhA crystal structure (2NSD) active site having *N*-(4-methylbenzoyl)-4-benzylpiperidine compound as a co-crystal ligand. The InhA active site comprised of many hydrophobic residues such as Gly96, Met155, Tyr158, Met161, Pro193, Met199, Ile202, Val203, Leu218, and Trp222. For each ligand at most 30 conformers were generated in the active site and out of these five poses per ligand were subjected to post-docking minimizations. Finally 100 compounds were selected for antibacterial assay based on their G-score, binding mode, and on visual inspection.

3.3. Biological assay of selected compounds

Compounds selected from docking studies were purchased from chemdiv vendor for their in vitro antitubercular activities against *M. tuberculosis* H37RV strain. These were purchased on the basis of their more than 90% purity claimed by the vendor (www.chemdiv.com), (NMR spectras are shown in [Supplementary data](#)). Only 80 compounds were available from database for their in vitro inhibitory concentrations determination. The minimum concentrations of the compounds for the complete inhibition of the bacterial growth per spot (minimum inhibitory concentration, MIC) were

determined and reported in [Table 3](#). Rifampicin was used as a reference compound and it showed the MIC value of 0.010 μ M. Among the selected hits, virtual hit VH07 exhibited biological activity at 2 μ g/ml whereas compound VH04 showed activity at 4 μ g/ml. Similarly five compounds showed antibacterial activity at 32 μ g/ml, 10 showed at 64 μ g/ml, 18 showed at 128 μ g/ml and remaining showed at more than 128 μ g/ml. The antibacterial activities of these more and less potent hits are summarized in [Table 3](#). The variations in the potencies of virtual screening hits might be due to the different membrane permeability of each compound and its extrusion from the bacterial cell by the efflux pump mechanism.

3.4. Binding mode elucidation of active hits

To obtain structural insights into the inhibitory mechanism by newly identified active compounds, their binding modes in the InhA active site were investigated. The predicted binding modes of highly potent molecules VH07 and VH04 are described in [Figures 5 and 6](#), respectively. The published literature reveals that crystal structures of InhA with different ligands have similar binding mode as that of the newly discovered antitubercular agents. On comparison of both of these compounds with the published InhA-NAD⁺ triclosan, diphenyl ethers, and arylamide reveal the same hydrogen bonding pattern with the –OH of NAD⁺ substrate and conserved amino acid Tyr158, a catalytic residue in the fatty acid reduction reaction ([Figs. 5 and 6](#)). The highest potency of VH07 hit in our virtual screening is probably due to the one extra hydrogen bonding between –OH group of its phenyl ring and carbonyl moiety of Gly96 backbone. In [Figure 5](#), it is obvious that t-type π – π interactions of both terminals phenyl rings with Phe97 and Phe149 might be responsible for more antitubercular activity compared to the other existing antitubercular agents. Similarly the second highly active hit, VH04 also acquires the same binding confirmation as that of VH07 and other co-crystal ligands. This bound conformation in active site is stabilized by the combination of different hydrogen bonds with the side chain –OH of Tyr158 and two H-bonds with pentose of NAD⁺ substrate already stacked in the crystal structure ([Fig. 6](#)). The lipophilic sites of these hits are also well gorged in the hydrophobic pockets of the active site for probable contribution to their high activity.

4. Conclusion

In this paper we applied the hybrid virtual screening protocol through the similarity search of highly active compounds followed by the molecular docking simulations to identify new and more potent antitubercular agents. Initially we used FCFP₄ fingerprints in similarity search which yielded the most of compounds having the conserved fragment (carbonyl) that is responsible for H-bonding interactions with the InhA. In second step after docking studies and biological assay, we have identified the two new antitubercular agents with their MIC, 2 μ g/ml and 4 μ g/ml from chemdiv database which is the more than twofolds from starting MIC value against H37RV antitubercular strain. Therefore we believe that this approach is helpful to identify the new hits with better activity profile against *M. tuberculosis*.

Acknowledgements

This work was supported by Korea Functional Proteomic Center, 21C Frontier Program of Korea Ministry of Education, Science and Technology and Grants from Korea Institute of Science and Technology (2E21590).

Supplementary data

Supplementary data associated with this article can be found, in the online version, at [doi:10.1016/j.bmc.2010.07.010](https://doi.org/10.1016/j.bmc.2010.07.010). These data include MOL files and InChIKeys of the most important compounds described in this article.

References and notes

1. Kaufmann, S. H. E.; McMichael, A. J. *Nat. Med.* **2005**, *11*, 578.
2. Agdamag, D. M. D.; Kageyama, S.; Solante, R.; Espantaleon, A. S.; Sangco, J. C. E.; Suzuki, Y. *Int J Tuberc. Lung Dis.* **2003**, *7*, 1104.
3. Ambrose, P. G.; Bhavnani, S. M.; Rubino, C. M.; Louie, A.; Gumbo, T.; Forrest, A.; Drusano, G. *Clin. Infect. Dis.* **2007**, *44*, 624.
4. Zhao, X. B.; Yu, H.; Yu, S. W.; Wang, F.; Sacchettini, J. C.; Magliozzo, R. S. *Biochemistry* **2006**, *45*, 4131.
5. Spigelman, M.; Gillespie, S. *Lancet* **2006**, *367*, 945.
6. Mdluli, K.; Spigelman, M. *Curr. Opin. Pharmacol.* **2006**, *6*, 459.
7. Banerjee, A.; Dubnau, E.; Quemard, A.; Balasubramanian, V.; Um, K. S.; Wilson, T.; Collins, D.; Delisle, G.; Jacobs, W. R. *Science* **1994**, *263*, 227.
8. Rozwarski, D. A.; Vilcheze, C.; Sugantino, M.; Bittman, R.; Sacchettini, J. C. *J. Biol. Chem.* **1999**, *274*, 15582.
9. Parikh, S. L.; Xiao, G. P.; Tonge, P. J. *Biochemistry* **2000**, *39*, 7645.
10. Wang, F.; Langley, R.; Gulten, G.; Dover, L. G.; Besra, G. S.; Jacobs, W. R.; Sacchettini, J. C. *J. Exp. Med.* **2007**, *204*, 73.
11. He, X.; Alian, A.; Stroud, R.; de Montellano, P. R. O. *J. Med. Chem.* **2006**, *49*, 6308.
12. Lu, H.; Tonge, P. J. *Acc. Chem. Res.* **2008**, *41*, 11.
13. Freundlich, J. S.; Wang, F.; Vilcheze, C.; Gulten, G.; Langley, R.; Schiehsler, G. A.; Jacobus, D. R.; Jacobs, W. R.; Sacchettini, J. C. *ChemMedChem* **2009**, *4*, 241.
14. Hea, X.; Alian, A.; de Montellano, P. R. O. *Bioorg. Med. Chem.* **2007**, *15*, 6649.
15. Kogej, T.; Engkvist, O.; Blomberg, N.; Muresan, S. J. *Chem. Inf. Model.* **2006**, *46*, 1201.
16. Verdonk, M. L.; Mortenson, P. N.; Hall, R. J.; Hartshorn, M. J.; Murray, C. W. *J. Chem. Inf. Model.* **2008**, *48*, 2214.
17. Pipeline Pilot Version 7.4; SciTegic, San Diego, CA, 2009.
18. Hassan, M.; Brown, R. D.; Varma-O'Brien, S.; Rogers, D. *Mol. Divers.* **2006**, *10*, 283.
19. Collins, L. A.; Franzblau, S. G. *Antimicrob. Agents Chemother.* **1997**, *41*, 1004.
20. Fells, J. I.; Tsukahara, R.; Liu, J. X.; Tigyi, G.; Parrill, A. L. *Bioorg. Med. Chem.* **2009**, *17*, 7457.
21. Cavasotto, C. N.; Abagyan, R. A. *J. Mol. Biol.* **2004**, *337*, 209.
22. Zhang, Y.; Skolnick, J. *Nucl. Acids Res.* **2005**, *33*, 2302.